THE ANALYSIS OF EMISSION LINES

A Meeting in Honour of the
70th Birthdays of D. E. Osterbrock & M. J. Seaton

Proceedings of the Space Telescope Science Institute Symposium,
held in Baltimore, Maryland
May 16–18, 1994

Edited by

ROBERT WILLIAMS
Space Telescope Science Institute, Baltimore, MD

MARIO LIVIO
Space Telescope Science Institute, Baltimore, MD

Ultraviolet Spectroscopy

By REGINALD J. DUFOUR

Department of Space Physics & Astronomy, Rice University, Houston, TX 77251-1892

A review of the field of astronomical ultraviolet spectroscopy with emphasis on *emission lines* in astrophysical plasmas is presented. A brief history of UV spectroscopy instruments is given, followed by a discussion and tabulation of major atlases of UV emission-line objects to date (mid-1994). A discussion of the major diagnostic UV emission lines in the $\sim$ 912–3200Å spectral region that are useful for determining electron densities, temperatures, abundances, and extinction in low- to moderate-density plasmas is given, with examples of applications to selected objects. The review concludes by presenting some recent results from HST, HUT, and IUE on UV emission-line spectroscopy of nebulae and active galaxies.

1. Introduction

The history of ultraviolet (UV) spectroscopy in astronomy spans over three decades now and such observations have led to many discoveries regarding the physical nature of the entire gambit of astronomical objects. Hot astrophysical plasmas have line and continuum emission and absorption processes for which UV spectroscopy can probe the more energetic physical processes that cannot be studied adequately in the optical or infrared. In addition, studies of the UV spectral properties of cooler bodies, such as planetary atmospheres, comets, and interstellar dust provide important information on their physical state and composition.

This article concentrates on reviewing some of the techniques and results from the study of *emission lines* in astronomical UV spectroscopy. Given that the range of astronomical objects from the Earth's geocorona to quasars show UV emission lines and that during the past three decades over two thousand papers have appeared in the literature, including numerous conferences and books, a comprehensive review is unpractical. Therefore, the author will limit this discussion to a review of the various emission-line diagnostics present in UV spectra from approximately the Lyman Limit (912Å) to near the atmospheric cutoff (3200Å). In addition, he will concentrate on recent results during the past few years obtained with the International Ultraviolet Explorer (IUE), the Hubble Space Telescope (HST), and the Hopkins Ultraviolet Telescope (HUT) flown on the 1991 Astro-1 space shuttle mission. Readers who wish to obtain a more comprehensive review of the observations and scientific results from UV spectroscopic studies across the entire repertoire of astronomical objects should began with a study of the book *Exploring the Universe with the IUE Satellite* (Kondo 1987), which contains 36 review articles on UV spectroscopic results for all types of astronomical objects, as well as discussions on the history and future promise of astronomical UV studies.

A good indicator of scientific interest in the field of astronomical UV spectroscopy during the past two decades can be derived from counting the numbers of scientific papers in the *Astrophysical Journal* under the subject keyword "ultraviolet astronomy" which was instigated in 1972. A plot of the numbers during the 1972–1993 period is shown in Figure 1. It shows that during the period 1972 to 1985 that the number of refereed papers on the subject increased from $\sim$25/yr to $\sim$100/yr, then dropped to about $\sim$65/year in the late 1980's, but increased rapidly to the $\sim$100 level again during the early 1990's. I interpret this trend as indicating that the "short-term" scientific
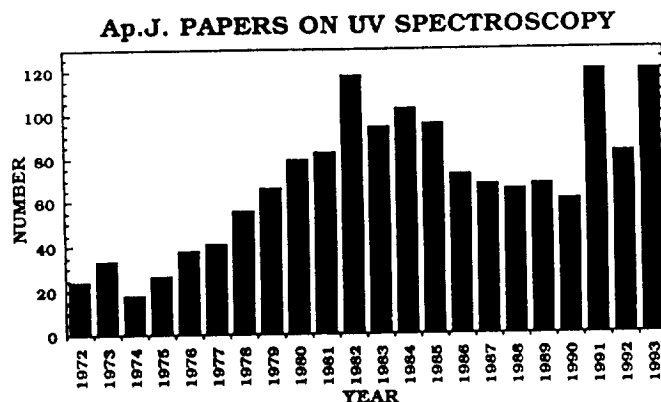
Ap.J. PAPERS ON UV SPECTROSCOPY

FIGURE 1. Graph of *Astrophysical Journal* papers on "UV Spectroscopy" during 1972–1993.

investigations with the IUE peaked in the mid-1980's and then dropped due to relatively longer time-scale multi-year project research with that satellite, then the rapid rise during the 1991–1993 period was due to the first scientific results from HST and HUT being published. I suspect that during the remaining part of the decade that ApJ publications related to UV spectroscopy will remain at the ~100/yr level due to additional results from IUE-HST-HUT observations and archival research are published, as well as results from EUVE and several UV astronomy space shuttle payloads recently flown or are planned. Not treated in this analysis are papers in the AJ, PASP, or European journals, which collectively add about 50% more to the total of refereed papers per year; or various conferences on spacecraft results or restricted astronomical topics, which probably add another 50% to the numbers of papers per year again.

2. A brief history of UV spectroscopy instruments

Astronomical UV spectroscopic studies began in the early 1960's with rocket flights. The first measurements of the UV continuum spectra of stars were obtained in 1961 with a low resolution objective grating spectrometer launched in an Aerobee rocket (Stecher & Milligan 1962). The first successful UV spectral line studies were made using a similar rocket-borne spectrometer in 1965 (Morton & Spitzer 1966). Subsequent rocket-borne UV spectrometers made the first observations of UV emission lines in hot stars and late-type supergiants. The late-1960's heralded the coming of the series of Orbiting Astronomical Observatories (OAOs), which were satellites specifically directed at obtaining imagery and spectroscopy of astronomical objects in the UV. Four OAO's were built during the late 1960's, and while two (OAO-A and OAO-B) were failures, OAO-2 (a reconstituted clone of OAO-A), was successfully launched in 1968 and was notable in initiating the era of UV spectroscopy from space-borne observatories. OAO-2 carried low-dispersion spectrometers for observations in the 1200–1400Å wavelength range and made hundreds of observations of astronomical sources during its three-year lifetime. A summary of the many scientific results of OAO-2 can be found in NASA SP-310 (Code 1972).

Astronomical UV spectroscopy in decade of the 1970's flourished with a variety of observations made from rockets, balloon-borne telescopes, manned-spacecraft, and un-

manned orbiters. The decade also marked the beginning of active European involvement in the field of UV spectroscopy. Notable European successes during this period included a rocket flight obtaining (for then) high resolution UV spectra of the W-R stars γ Vel and ζ Pup over the 900–2300Å region, two balloon-borne high resolution UV spectrometers working in the 2000–3000Å region accessible in the upper atmosphere, and two satellites—TD-1 (ESRO) & ANS (Netherlands), which obtained UV imagery and low resolution spectroscopy of many astronomical sources. The two most notable US instruments for astronomical UV spectroscopy during the decade were the launch of the COPERNICUS (OAO-C) satellite in 1972 and the International Ultraviolet Explorer (IUE) in 1978. The COPERNICUS satellite, developed at Princeton (Rogerson *et al.* 1973), obtained moderate- and high-resolution UV spectra of hundreds of bright stars during its two-year lifetime. Though its single-channel stepping spectrometer limited the practical wavelength coverage in a given observation, the signal-to-noise on the high resolution ($\sim$0.1Å) UV spectra of bright stars obtained by COPERNICUS surpassed anything previously, and it made important contributions to studies of stellar mass-loss and interstellar abundances from observations of various UV resonance absorption and emission lines.

In astronomical UV spectroscopy, the decade of the 1980's clearly belongs to the IUE satellite. Launched on 26 January 1978 into a geosynchronous orbit by a Thor-Delta rocket, the IUE was developed as an international collaborative effort by NASA-SRC-ESA with its sole mission being UV spectroscopy of astronomical bodies over the $\sim$ 1150–3300Å wavelength range (Boggess *et al.* 1978). Composed of a 0.45m Richey-Crétien telescope with two echelle spectrographs and four SEC Vidicon detectors, the IUE has obtained over 100,000 spectra of astronomical objects and continues to operate to date, some 13 years beyond its designed 3-year lifetime ("*...and keeps going...*"—IUE's motto these days). IUE operates in two modes: a high-resolution mode, whereby "short wavelength" (1145–1930Å continuous coverage) and "long wavelength" (1845–1920Å continuous coverage) two dimensional echelle spectra are imaged by one of three (SWP and LWP or LWR, respectively) SEC Vidicon cameras with UV converters; and a low-resolution mode, whereby the cross-disperser grating is removed and a single spectrum is imaged over the 1150–1975Å range with the SWP camera and over the 1910–3300Å region with the LWP/R cameras (Harris & Sonneborn 1987). At high resolution, the point-source resolution is about 0.1–0.2Å (decreasing with longer wavelengths) for the SWP range and about 0.2Å for the LWP/R range; at low resolution, the corresponding resolution varies from 3–7Å with the SWP and $\sim$6Å with the LWP/R cameras. One of the main limitations of the IUE, particularly for emission-line studies, is dynamic range—its A-D converter is only 8-bits (0–255), and the best signal-to-noise (S/N) possible is only 25–30 for multiple exposures and typically only 15–20 on single long exposure spectra (due to a combination of fixed-pattern noise, reseaux marks, and radiation "hits").

The decade of the 1990's heralded the promise of a "new era" in astronomical UV spectroscopy; beginning with the launch of the Hubble Space Telescope (HST) on 24 April 1990. Compared to IUE, HST offered the increased power of a larger aperture (2.4m vs. 0.45m) and higher sensitivity and dynamic range (12-bit vs. 8-bit encoded data) in its spectroscopic instruments for UV spectroscopy. In addition, when the primary mirror aberration problem was discovered, more priority was given to spectroscopy projects than previously anticipated. Thus HST made an immediate impact on the field of astronomical UV spectroscopy, particularly regarding emission line studies. Two of the five original axial science instruments on HST are spectrographs with UV capabilities: FOS (Faint Object Spectrograph) and GHRS (Goddard High Resolution Spectrograph). Both have a variety of gratings for spectroscopy over the 1150–8500Å wavelength range (FOS) and

Instrument	Projected Aperture Size	Resolving Power ($\lambda/\Delta\lambda$)	Time Resolution	Wavelength Range (Å)	Magnitude Limit
FOS	0.085″–3.7″	1,300	30 ms	1150–8500	13.7–20.5–20.2
		250	30 ms	1150–8500	15.3–22.9–21.5
GHRS (Side 1)	0.22″, 1.74″	80,000	50 ms	1150–1700	11–14
		25,000	50 ms	1100–1900	13–16
		2,000	50 ms	1100–1900	17
(Side 2)		80,000	50 ms	1700–3200	11–14
		25,000	50 ms	1150–3200	13–16

TABLE 1. HST UV spectroscopy capabilities

the 1100–3200Å range (GHRS) at a variety of resolutions. Detailed capabilities of these two instruments are listed in Table 1. While the larger aperture of HST is somewhat offset by the small apertures of spectrographs compared to IUE for extended targets, the potential S/N of UV spectroscopy observations with HST exceed that possible with IUE by 1–2 orders of magnitude. In addition, the maximum resolution of GHRS in the far-UV exceeds that of IUE by a factor of about 7 (*cf.* the recently published review by Brandt *et al.* 1994 on instrumental characteristics and a summary of early science results from GHRS).

In December 1990 the Astro-1 space shuttle mission (STS-35) carried into orbit three UV telescopes for imaging (UIT) and spectroscopy (HUT and WUPPIE). The Wisconsin Ultraviolet Photo-Polarimeter Experiment (WUPPIE) is a 0.5m f/10 Cassegrain telescope with a spectropolarimeter for simultaneous observations of the UV energy distribution and polarization over the 1400–3200Å region at 12Å resolution. The Hopkins Ultraviolet Telescope (HUT) is a 0.9m f/2 telescope with a prime-focus spectrograph capable of UV spectroscopy over the 830–1860Å range with a nominal resolution of ∼3Å (Davidsen *et al.* 1992). A noteworthy accomplishment during this mission was by HUT obtaining high S/N UV spectra of a variety of faint emission line nebulae and galaxy nuclei in the 830–1150Å region, which previously had not been observed by UV spectrographic instruments. Compared to previous UV spectroscopy instruments, the large aperture, short f-ratio optics, and large slit sizes of HUT enabled high S/N spectra of faint nebulosities to be obtained in relatively short exposures.

While HUT on Astro-1 made spectroscopic observations shortward of the 912Å Lyman limit, generally referred to as the "extreme ultraviolet," the era of EUV astronomy really began with the launch of the Extreme Ultraviolet Explorer satellite (EUVE) in 1992 June. In addition to imagery in the EUV, the satellite is equipped with a spectrometer which covers the 70–760Å region at a resolution of R ∼ 250. EUV spectroscopy observations began in mid-1993, after completion of an all-sky survey in four EUV bandpasses (60–180Å, 160–240Å, 345–605Å, and 500–740Å), and the first spectroscopic results are beginning to appear in the literature at the time of writing (Bowyer 1994).

The remainder of the decade looks bright for UV spectroscopy as HST, IUE, and EUVE continue to operate, a second Astro mission is planned for 1995, several UV imagery and spectroscopy instruments are planned for the space shuttle (*e.g.*, ORFEUS, Krämer *et al.* 1990) and rocket flights, and the Far-Ultraviolet Spectroscopic Explorer (now called LYMAN) may be launched into orbit before the decade is over. LYMAN will possibly be the next major orbiting UV spectroscopy mission (though plans for a Russian 1.7m UV spectroscopy telescope were announced in 1990), and is planned to consist

The IUE Ultraviolet Spectral Atlas 1983, Wu *et al.*, IUE Newsletter No. 23.

The IUE Ultraviolet Spectral Atlas, Addendum I 1991, Wu *et al.*, IUE Newsletter No. 43.

IUE Ultraviolet Spectral Atlas of Selected Astronomical Objects 1992, Wu *et al.*, IUE Reference Publication 1285.

IUE Spectral Atlas of Planetary Nebulae, Central Stars, and Related Objects 1988, Feibelman *et al.*, NASA Reference Publication 1203.

An Ultraviolet Atlas of Quasar and Blazar Spectra 1991, Kinney *et al.*, ApJ Suppl. 75, 645.

An Atlas of Ultraviolet Spectra of Star-Forming Galaxies 1993, Kinney *et al.*, ApJ Suppl. 86, 5.

Ultraviolet Spectra of QSO's, BL Lacertae Objects, and Seyfert Galaxies 1993, Lanzetta, Turnshek & Sandoval, ApJ Suppl. 84, 109.

IUE-ULDA Access Guide No. 1: Dwarf Novae and Nova-like Stars 1989, La Dous, ESA SP 1114.

IUE-ULDA Access Guide No. 2: Comets 1990, Festou, ESA SP 1134.

IUE-ULDA Access Guide No. 3: Normal Galaxies 1992, Longo & Capacioli, ESA SP 1152.

IUE-ULDA Access Guide No. 4: Active Galactic Nuclei 1993, Courvoisier & Paltani, ESA SP 1153A & 1153B.

TABLE 2. Some selected atlases of UV emission-line objects

of a meter-class telescope for dedicated UV *two-dimensional* spectroscopy at moderate resolution in the EUV (100–912Å) and high resolution in the FUV (912–1200Å) (Moos 1990). In addition, in the 1996–1997 period we will have the second HST refurbishment mission, which will install STIS (Space Telescope Imaging Spectrograph), enabling two-dimensional UV-optical spectroscopy to be done with HST.

3. Reference catalogs and atlases

One of the greatest scientific benefits of the long lifetime of the IUE satellite is that it has accumulated over 100,000 UV spectra of astronomical objects covering the 1150–3200Å wavelength range. Such an extensive data archive provides the opportunity to produce extensive compilations of UV spectra of various classes of astronomical objects for the first time. The first efforts to produce atlases of the UV spectra of astronomical objects were made by Benvenuti *et al.* (1982) on supernovae, by Wu *et al.* (1983) and Heck *et al.* (1984) on normal stars, and by Rosa *et al.* (1984) on extragalactic H II regions. During the past several years a number of extensive atlases have appeared, and several that are most relevant to studies of UV emission line spectra are listed in Table 2. A more complete listing of all IUE-related UV spectra atlases to late 1993 is given by Pitts (1993) in IUE Newsletter No. 50.

The four IUE-ULDA "access guides" published by ESA utilize the *Uniform Low Dispersion Archive* of IUE spectra (ULDA) and an access and analysis software package called USSP (Wamsteker *et al.* 1989). The guides are directed towards specific classes of astronomical objects, and contain all of the good UV spectra taken of each class through 1991; while the ULDA/USSP archive and software are intended to provide archive users with a current easily accessible processed dataset and software for analysis of IUE low dispersion spectra. By contrast, the Kinney *et al.* (1991, 1993) atlases present low dis-

person spectra of galaxies that are processed with a continuum weighted extraction technique (called *optimal*) that is designed to improve S/N. Since Kinney *et al.* required there be at least three good SWP or LWP/R spectra of each object for inclusion, their atlases contain only a subset of the existing IUE spectra archive on each class of object. They also include references to previous studies of many of the individual objects. This spectral extraction technique results in significant S/N improvements in some spectra over the old "boxcar" processing. Recently, Lanzetta *et al.* (1993) published an atlas of optimal-extracted spectra of QSO's, BL Lac objects, and Seyfert galaxies, which supplements the original Kinney *et al.* 1991 atlas by removing the "3-good spectra" requirement and contained an additional 192 objects compared to the 69 in the original Kinney *et al.* atlas.

All UV spectroscopists will benefit from having a copy of NASA Reference Publication 1285, *IUE Ultraviolet Spectral Atlas of Selected Astronomical Objects* by Wu *et al.* (1992). This atlas includes spectral plots and tabular flux data on the spectra of some 330 astronomical objects ranging from the moon to quasar PKS 2344+092, covering the 1150–3200Å wavelength range, with many of the spectra (stellar and semi-stellar objects) extracted using a gaussian-weighted technique to improve S/N. In addition to the variety of objects with representative spectra, the atlas gives excellent lists of various UV emission and absorption lines in astrophysical spectra, as well as a brief discussion and tabulation of interstellar extinction in the UV. Of great importance and utility to current and future users of low dispersion IUE archive data is the discussion and tabulation of artifacts in IUE SWP and LWP/R spectra.

Figure 2 on the next page shows composite UV spectra of four strong emission line objects taken from the Wu *et al.* (1992) atlas: (a) the symbiotic star RR Telescopii, (b) the high excitation planetary nebula NGC 7027, (c) a bright filament in the Cygnus Loop supernova remnant, and (d) the nucleus of the Seyfert 2 galaxy NGC 1068. In the center of the figure is an identification strip listing some of the stronger UV lines and multiplets seen in all four spectra. While the four objects represent quite different physical conditions of ionization source, temperature, density, and size of the emitting region, it is noteworthy that the stronger UV emission lines are from the same ions.

It is important to note that, with regard to the large IUE UV spectra archive, all of the low dispersion SWP, LWP, and LWR spectra are currently being re-processed with an entirely new software package, called NEWSIPS, which entails a more rigorous geometric registration, image-transfer function, and absolute calibration based on white dwarfs (Nichols *et al.* 1994). In addition, the spectra are extracted using the optimal technique and the data are available in the astronomical FITS standard format. Pending continued NASA funding, this reprocessing will extend into high dispersion spectra as well. Significant S/N improvements are realized in many of the spectra over the old processing and the new extensive (and easily accessible via NASA NDADS) IUE UV spectra archive is expected to be of great scientific value for decades to come.

4. UV emission-line diagnostics

Over the 912–3200Å wavelength range hot astrophysical plasmas of standard (solar) composition emit a wealth of emission lines which can be used to determine electron temperatures (T_e), densities (N_e), and ionic concentrations $(N(X^i))$ in the plasma. These diagnostics can then be used with others in the optical and infrared to develop detailed photo-ionization and/or shock-ionization models of a given object. Some of the "classic" examples in the early literature of these techniques utilizing UV emission-line diagnostics in conjunction with observations at other wavelengths and models are Harrington *et al.*'s

(1982) study of the planetary nebula NGC 7662, Raymond *et al.*'s (1983) study of the Cygnus Loop supernova remnant, Hayes & Nussbaumer's (1986) study of the symbiotic star RR Tel, and Ferland & Osterbrock's (1986) study of Seyfert 2 galaxies. A good summary of some of the more important UV emission-line diagnostics, with plots of several useful line ratios, is the paper by Czyzak, Keyes, & Aller (1986); in addition, the textbooks of Aller (1984) and Osterbrock (1987) contain much information of UV emission-line diagnostics as well. While the early studies were classics in the techniques utilized, newer atomic data has since appeared in the literature for many of the UV-line ions which should be utilized in future studies.

A list of the many UV emission lines in the 1150–3200Å wavelength range found in IUE low dispersion spectra of all types of objects is given in the Wu *et al.* (1992) atlas. The stronger lines seen in the four objects of Figure 2 are: H I Lyα λ1216, N V $\lambda\lambda$1238–1242, Si IV+O IV]+S IV $\lambda\lambda$1394–1406, N IV] $\lambda\lambda$1483–87, C IV $\lambda\lambda$1548–1550, He II λ1640, O III] $\lambda\lambda$1658–67, N III] $\lambda\lambda$1747–1754, Si III] $\lambda\lambda$1883,92, C III] $\lambda\lambda$1907,9, [O III]+C II] $\lambda\lambda$2321–31, [O II] λ2470, Mg II $\lambda\lambda$2796–2803, and O III λ3133. A more detailed list of UV lines seen at high dispersion is found in Penston *et al.* (1983) for the symbiotic star RR Tel (but see also Doschek & Feibelman (1993) and Aufdenberg (1993) for an improved list in the ~1150–2000Å range). For expected emission lines in the EUV-FUV range, a useful reference is Doyle & Keenan (1992), which gives the results of theoretical calculations of line emissivities in the 100–2800Å wavelength range at densities appropriate to stellar sources.

Six physical processes give rise to the formation of emission lines in the ultraviolet: *(a) direct recombination*—electron capture and cascade processes are responsible for the strong He II Baα 1640Å and He II Paschen series seen in high excitation nebulae and the He I $2s^3P - np$ series (as well as Lyα); *(b) electron collisional excitation*—this gives rise to the "forbidden lines" corresponding to magnetic dipole and electric quadrupole transitions such as [Ne III] λ1815, [O III] $\lambda\lambda$2321+31, [O II] λ2470, and certain resonance transitions such as N V $\lambda\lambda$1238+42, C IV $\lambda\lambda$1548+50, and Mg II $\lambda\lambda$2796+2803; *(c) intercombination*—resulting in permitted (electric dipole) and forbidden (electric quadrupole or magnetic dipole) multiplets closely space in wavelength, such as N IV] $\lambda\lambda$1483–87, O III] $\lambda\lambda$1658–1667, N III] $\lambda\lambda$1747–54, Si III] $\lambda\lambda$1883–92, C III] $\lambda\lambda$1907+9, and C II] $\lambda\lambda$2325–2329 (lines that are among the strongest in UV spectra); *(d) dielectronic recombination*—important for many far-UV line multiplets such as C II λ1335, C III $\lambda\lambda$977+1176, N III λ991, N IV λ923, as well as many of the extreme UV lines of ions of the CNO elements, it can be important for many of the lines of CNO ions in the UV (*cf.* Nussbaumer & Storey 1984 for a thorough discussion and tabulation of the various lines); *(e) Bowen fluorescence*—gives rise to exceptionally strong lines of O III (compared to simple recombination) at 2837Å, 3023Å, 3045Å, and particularly 3133Å, in the near-UV spectra of high excitation planetary nebulae and symbiotic stars; and *(f) charge exchange*—important for determining the ionization equilibrium near ionization fronts, it also can affect the low-level populations of metastable ions like [O II] and [S II]. Williams (1994) gives an interesting chart of various emission lines from these processes for ions of astrophysical interest in this volume.

In nebular plasmas, the level populations of a given ion are determined by the equilibrium between radiative decay and collisions to/from a given excited level i and other levels j. The statistical equilibrium equations (Osterbrock 1989, p. 57) take the form:

$$\sum_{j\neq i} n_j N_e q_{ji} + \sum_{j>i} n_j A_{ji} = \sum_{j\neq i} n_i N_e q_{ij} + \sum_{j<i} n_i A_{ij}, \tag{1}$$

with the left hand side giving transitions populating level i and the right hand side giving
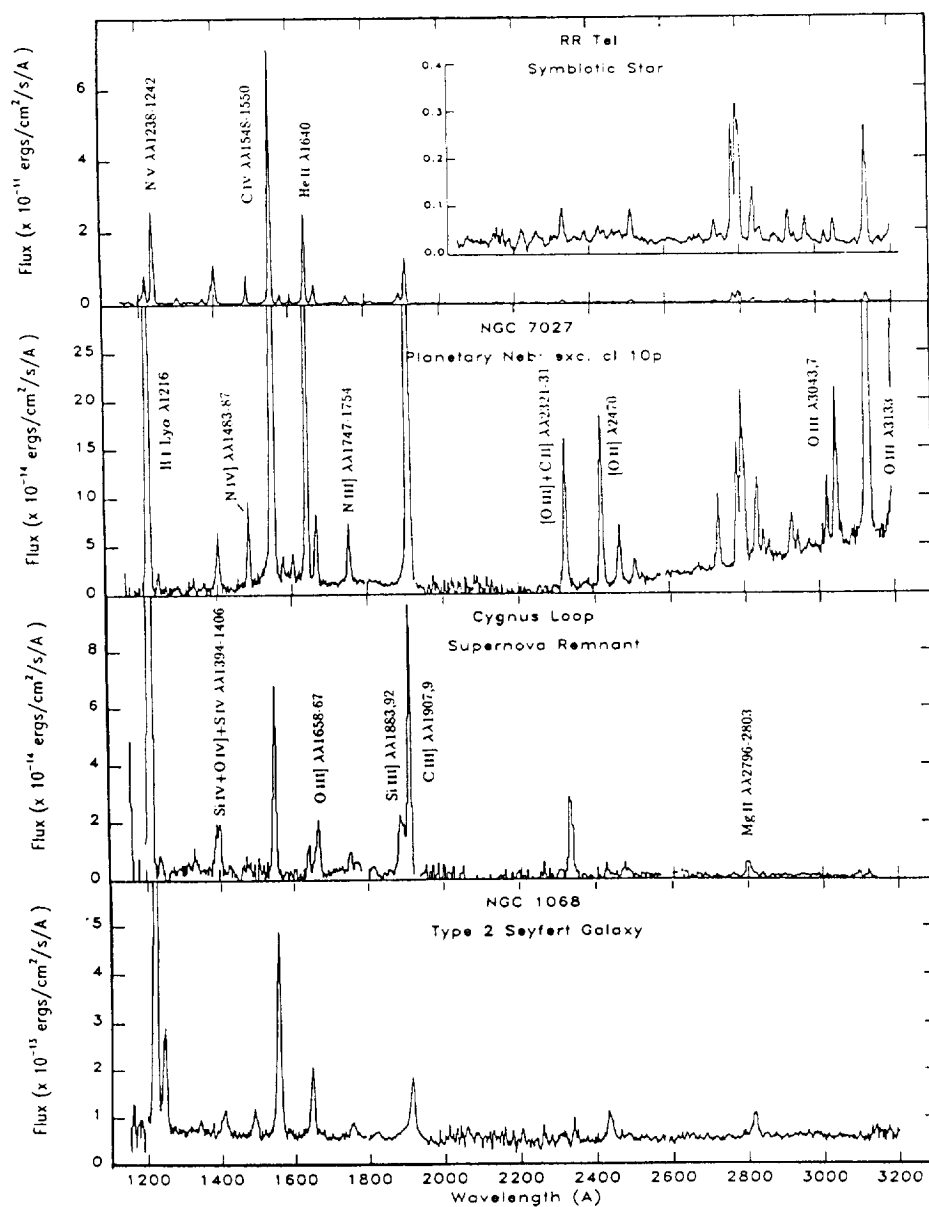
FIGURE 2. Example IUE low dispersion spectra of selected emission-line objects adopted from the atlas of Wu *et al.* (1992)

transitions that depopulate level i. A_{ij} are the radiative transition probabilities for $i \rightarrow j$ (to all lower levels) and q_{ij} are the collisional excitation/deexcitation rates for level i. For $i > j$, the collisional deexcitation rate is:

$$q_{ij} = \frac{8.63 \times 10^{-6}}{\sqrt{T_e}} \frac{\Omega(j, i)}{\omega_j},$$
(2)

and for $j < i$, the collisional excitation rate can be written:

$$q_{ji} = \frac{\omega_j}{\omega_i} q_{ij} e^{-E_{ij}/kT_e},$$
(3)

where Ω is the relevant collision strength (which have only a weak dependence on T_e), the ω's are the relevant statistical weights, E_{ij} is the energy of level i above j (normally the ground level), and T_e is the electron temperature. The emissivity of the $i \rightarrow j$ transitions can then be written as

$$4\pi I_{ij} = A_{ij} N(X^i) n_i E_{ij},$$
(4)

where $N(X^i)$ is the ionic abundance, n_i is the fractional level population, and E_{ij}. Therefore, the emissivity (or observed intensity) ratio of two excited levels physically depend on how the two level populations are influenced by collisional processes that populate and depopulate the two levels. When collisional deexcitation rates for the two levels are very different the line ratio is density sensitive; when collisional excitation rates for the two levels are very different the line ratio is temperature sensitive.

4.1. Density diagnostics

Emission line ratios of two metastable transitions from upper levels of similar excitation energy to a given lower level are useful diagnostics of electron density when the lifetimes of the upper levels are significantly different and the plasma density is near the "critical density" of the longer lived level. For a given level i, the critical density is:

$$N_c(i) = \sum_{j<i} A_{ij} / \sum_{j \neq i} q_{ij},$$
(5)

where A_{ij} is the radiative transition probabilities for $i \rightarrow j$ (to all lower levels) and q_{ij} are the collisional excitation/deexcitation rates for level i.

Since collisional excitations have an energy threshold, but collisional deexcitations do not, the collisional deexcitation-to-radiative decay rate for an excited level is relatively insensitive to T_e (eqn. 5). Therefore, radiative decay from multiplet excited levels of a given ion with similar excitation energies to a common lower level are predominantly sensitive to level lifetimes (given comparable collisional deexcitation rates), and thus are good diagnostics of electron density over a limited range of density near the critical densities of the longer-lived upper level. For $N_e \ll N_c$ for any two multiplet levels, their intensity ratio is effectively equivalent to the ratio of collision strengths (low density limit condition). By contrast, when $N_e \gg N_c$, the intensity ratio is fixed by the ratio of statistical weights and transition probabilities (the high density limit condition, where LTE applies rigorously).

At optical wavelengths, the $^2D-^4S$ ground transition doublet for np^3 ions of [O ii] and [S ii] (and to a lesser extent [N i], [Cl iii], [Ar iv], and [K v]) have been used as density indicators in nebulae. In the UV, the [Ne iv] $\lambda2422/\lambda2424$ doublet can be used as a density diagnostic for high excitation objects like planetary nebulae and supernova remnants. However, the UV is special in that intercombination lines of C ii], C iii], N iii], O iv], and Si iii] exist and provide density diagnostics for nebulae, particularly at higher densities ($> 10^4$ cm^{-3}) appropriate for symbiotic stars, proto-PN, and HH-objects.

Of particular utility are the $^3P_{1,2}-{}^1S_0$ doublets of C III] and Si III] which are in the $\lambda \sim 1900$ spectral region. The doublets consist of a highly forbidden magnetic quadrupole transition ($nsnp\ ^3P_2-{}^1S_0$ C III] 1906.8Å & Si III] 1882.7Å) and an intercombination, or "semi-forbidden" electric dipole transition ($nsnp\ ^3P_1 - ns^2\ ^1S_0$ C III] 1908.6Å & Si III] 1892.0Å). As the density increases, the shortward forbidden line is more collisionally quenched and the ratios of $\lambda1907/\lambda1909$ and $\lambda1883/\lambda1892$ decrease from a low-density limit ratio of ~1.5 (set by the ratio of collision strengths) to a high-density limit ratio of "near zero" (set by the ratio of statistical weights and transition probabilities. Plots of these two ratios are given in Figure 3, taken from the recent study by Keenan, Feibelman, & Berrington (1992) which uses more modern atomic data than previous investigations. Note that the C III] doublet is a good density indicator over the $3 \times 10^3 \leq N_e \leq 2 \times 10^5$ cm^{-3} range, while the Si III] is a good indicator for higher densities, $3 \times 10^4 \leq N_e \leq 3 \times 10^{10}$ cm^{-3}. The ratios are very insensitive to T_e, as can be seen in Fig. 3, where the four lines represent the ratio for $T_e = 5000$ K (*short-dashed line*), 10,000 K (*solid line*), 15,000 K (*long dashed line*), and 20,000 K (*dashed-dotted line*). Another doublet in the UV useful for density diagnostics in highly excited plasmas is N IV] $\lambda1486.5/\lambda1483.3$, which increases by over four orders of magnitude in the range $10^6 \leq N_e \leq 10^{11}$ cm^{-3} (Czyzak *et al.* 1986).

The N III] $2s^22p^2P - 2s2p^2\,^4P$ intercombination multiplet near $\lambda \sim1750$Å (1746.8Å, 1748.7Å, 1749.7Å, 1754.0Å, and 1752.2Å lines) provides several density-sensitive line ratio diagnostics (Czyzak *et al.* 1986; Keenan *et al.* 1994) which can be exploited with high resolution UV spectra. Czyzak *et al.* presented plots of three N III] density diagnostic line ratios: N III] $\lambda1752.2/\lambda1749.7$ is useful over both a low density range ($\sim 100 - 3000$ cm^{-3}) and over a high density range ($\sim 10^8 - 10^{10}$ cm^{-3}); similarly, the N III] $\lambda1754.0/\lambda1749.7$ ratio is a good diagnostic over two density ranges, for $N_e < 3000$ cm^{-3} and for $10^9 \leq N_e \leq 3 \times 10^{11}$ cm^{-3}; thirdly, the N III] $\lambda1748.7/\lambda1752.2$ ratio is useful in the high density range $3 \times 10^8 \leq N_e \leq 3 \times 10^{11}$ cm^{-3}. Keenan *et al.* (1994) noted four useful density diagnostic line ratios of N III]: $\lambda1754.0/\lambda1749.7$, $\lambda1752.2/\lambda1749.7$, $\lambda1748.6/\lambda1749.7$, and $\lambda1746.8/\lambda1749.7$, and discussed the effects of using modern atomic data (collision strengths and oscillator strengths) for N III on the line ratio diagnostics. They presented plots of two ratios, $\lambda1754.0/\lambda1749.7$ and $\lambda1752.2/\lambda1749.7$, computed with the modern atomic data and compared to the older results of Czyzak *et al.* (1986). These two plots are reproduced in Figure 4. They note that the newer atomic data results in difference as much as 24% in the line ratios for lower densities.

The intercombination multiplets of C II] near $\lambda \sim2325$Å (2323.5Å, 2324.7Å, 2325.4Å, 2326.9Å, and 2328.1Å) and O IV] near $\lambda \sim1400$Å (1397.2Å, 1399.8Å, 1401.2Å, 1404.8Å, and 1407.4Å) are similar to that of N III] and provide comparable sets of density diagnostics. However, both the C II] $\lambda\lambda2325$ and O IV] $\lambda\lambda1402$ multiplets are blended with lines from other ions ([O III] $\lambda2321.0$ & N II] $\lambda2325.9$ in the first case; and S IV] $\lambda1398.1, \lambda1404.8, \lambda1406.0$ & Si IV $\lambda1402.8$ in the second) which make measurements difficult even at high resolution. Figure 5 shows two plots of the regions of the O IV] and C II] lines from IUE high dispersion spectra of the symbiotic star RR Tel, which illustrates the resolution obtainable with IUE for a stellar object (extended nebulae have significantly degraded resolution with the large aperture). Observations of these multiplets in emission-line stars and nebulae with GHRS on the Hubble Space Telescope offer the promise of much improved wavelength resolution and photometric accuracy, as is illustrated at this meeting in the poster paper of Walter *et al.* (1994) for a GHRS spectrum of the C II] multiplet in the Orion Nebula.

Use of the UV C II], N III], and O IV] multiplets for density diagnostics is facilitated my the availability of modern collision strengths calculated over a wide range of temperatures
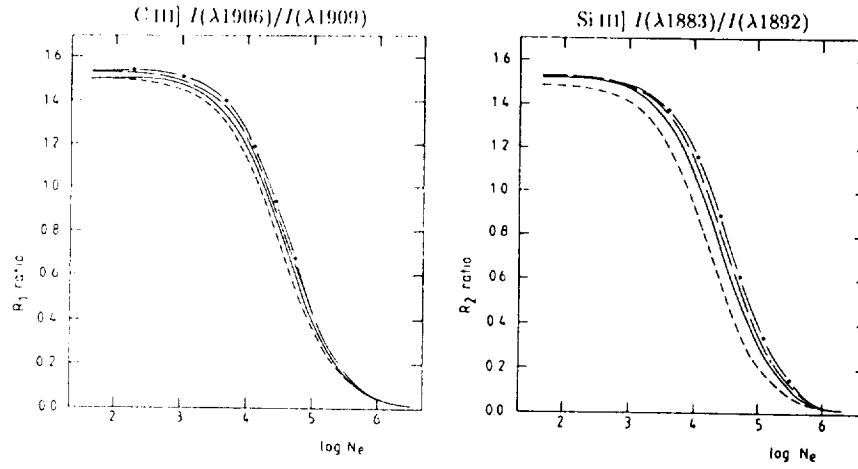
FIGURE 3. Plots of the N_e diagnostic line ratios of C III]$\lambda1907/\lambda1909$ (left) and Si III]$\lambda1883/\lambda1892$ (right) as a function of density N_e from Keenan et al. (1992).
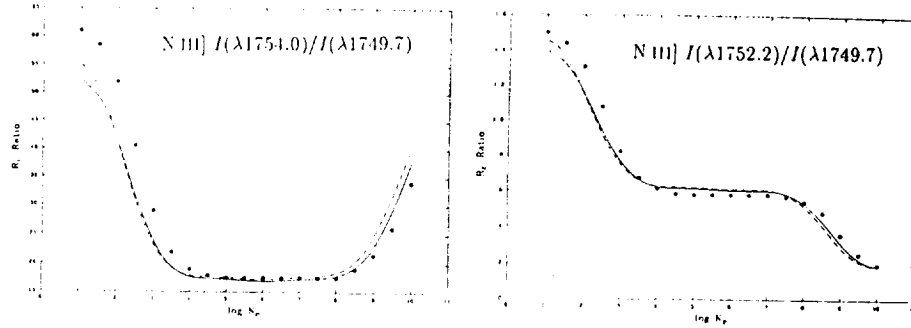
FIGURE 4. Plots of two N_e diagnostic line ratios of N III]: $\lambda1754.0/\lambda1749.7$ (*left*) and $\lambda1752.2/\lambda1749.7$ (*right*), taken from Keenan et al. (1994). Lines represent results for three T_e (5,000 K, 10,000 K, and 20,000 K) and the dots represent previous results based on older atomic data.

by Blum & Pradhan (1992) using an 8-state R-matrix method developed for the Opacity Project). However, for N III, Stafford, Bell & Hibbert (1994) derived collision strengths using an 11-state R-matrix code which differ from those of Blum and Pradhan by as much as 25% for $T_e = 10,000$ K. Therefore, observationalists who derive joy at being able to measure a line ratio to better than 10% with modern instruments need to be mellowed by the fact that the atomic data used to derive densities, or temperatures and abundances, are still uncertain at the 10–30% level. The review by Pradhan at this conference summarizes the best modern atomic data to date for use in emission-line diagnostics. Of particular note and usefulness is the recent compilation of collision strengths (and their weak, but important dependence on T_e) in Volume 57 of *Atomic*
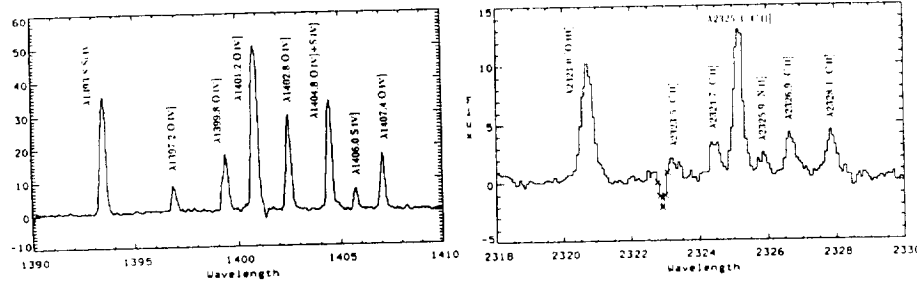
FIGURE 5. Plots of the O IV] 1402Å multiplet (*left*) and the C II] 2325Å multiplet (*right*) in RR Tel taken from archival IUE high dispersion spectra (SWP 29535 & LWR 2021).

Data and Nuclear Data Tables (1994 July issue). Hopefully, a future issue will have a similar compilation of oscillator strengths and transition probabilities for astrophysically interesting ions.

4.2. Temperature diagnostics

The ratio of two emission lines from an ion produced by radiative decay from levels which have significantly different excitation energies are primarily sensitive to the energy distribution of the free electron gas which populate the two levels by collisional excitation. This is due to the exponential dependence of the collisional excitation process (eqn. 3), which makes the level populations in the line emissivity equation (eqn. 4) strongly temperature dependent. To a good approximation, the ratio of line emissivities for two excited levels of energies $j > i$ can be written as (Aller 1984; Osterbrock 1989):

$$\frac{I_i}{I_j} = K \frac{(1 + ax)}{(1 + bx)} e^{\frac{-(E_i - E_j)}{kT_e}},$$

(6)

where K, a, and b are constants that depend on collision strengths and transition A-values, and $x = 10^{-2} N_e/\sqrt{T_e}$. For many lines a and b are $<< 1$, so at low densities (i.e. when $x < 1$) the ratio of two lines with significant different excitation energies have an exponential sensitivity to T_e.

Over the optical spectral region accessible to ground-based spectroscopy, "auroral-to-nebular" forbidden line ratios ($^1S_0 - {}^1D_2/{}^1D_2 - {}^3P_{1,2}$) of LS-coupled ground state configurations of np^2 ions such as [N II] $\lambda 5755/\lambda\lambda 6548 + 83$ and [O III] $\lambda 4363/\lambda\lambda 4959 + 5007$ have been used to derive T_e in nebulae, emission-line stars, and galaxies. Correspondingly, "transauroral" transitions from the $^1S_0$ level to the ^3P ground multiplet (the strongest transition being $^1S_0 - {}^3P_1$) have lines in the UV spectral region which can be used with the optical nebular transitions for temperature diagnostics. In addition, np^4 ions such as O I, Ne III, and Ar III have similar LS-coupled configurations with UV transauroral lines. A list of the UV transauroral lines and the corresponding nebular transition lines for eight ions prominent in nebular spectra is given in Table 3 (wavelengths taken from Osterbrock 1989).

In addition to the ground-state configuration transitions, intercombination transitions from $^5S_2 \rightarrow {}^3P_2$ and from $^5S_1 \rightarrow {}^3P_1$ produce UV lines that are observed in many nebular objects—particularly O III] 1660.8–1666.2Å & N II] 2139.0–2142.8. These intercombination lines can be compared to the usually strong lines of [O III] and [N II] to

Ion	Transauroral $(^3P_1 - {}^1S_0)$	Nebular $(^3P_2 - {}^1D_2)$	$R^*(\frac{Neb}{TrA})$
[N II]	3062.8	6583.4	1082
[O III]	2321.0	5006.9	762
[Ne V]	1575.2	3425.9	507
[S III]	3721.7	9530.9	753
[Ar V]	2691.1	7005.7	29.5
[O I]	2972.3	6300.3	680
[Ne III]	1814.6	3868.8	610
[Ar III]	3109.2	7135.8	64.4

*Line ratio computed for $N_e = 10^3$ cm^{-3} and $T_e = 10^4$ K

TABLE 3. UV/optical—transauroral/nebular line ratios for T_e determinations

derive T_e and are better high temperature diagnostics than the auroral and transauroral lines of [O III] and [N II]. Czyzak *et al.* (1986) and Keenan & Aggarwal (1987) present diagrams of the [O III]/O III] UV line ratio $(\lambda 2322)/(\lambda\lambda 1660+ 1666)$ versus T_e and of the O III]/[O III] UV-optical line ratio $(\lambda\lambda 1660+1666)/ (\lambda\lambda 4959+5007)$ versus the optical auroral-to-nebular [O III] $(\lambda 4363)/(\lambda\lambda 4959+5007)$ ratio. The Keenan & Aggarwal plots are based on more modern atomic data and are presented in Figure 6. The UV lines of O III] and N II] provide unambiguous determinations of T_e for $N_e < 10^5$cm^{-3} and, when combined with T_e results from the optical auroral-to-nebular transitions, can provide unique information on the extent of temperature fluctuations in gaseous nebulae. However, as noted by Nussbaumer & Storey (1984), if dielectronic recombination contributes to the ^5S levels in an object, then one will obtain elevated temperatures from the UV lines (and abundances).

Dielectronic recombination lines of several ions of the CNO element group exist in the UV and can be compared with collisionally excited lines for T_e determinations. The emissivity of a dielectronic line can be written as:

$$4\pi I_D(\lambda) = N_e N(X^{i+1})\alpha_D(N_e, T_e)E_\lambda, \tag{7}$$

where $\alpha_D(N_e, T_e)$ is the effective dielectronic recombination coefficient for the $X^{i+1}+e \rightarrow X^i + h\nu$ recombination process. The dielectronic recombination coefficient in eqn. (7) is relatively insensitive to density but has a temperature dependence which can be characterized roughly as $\sim T^{-3/2}exp[-E/kT]$. The ratio of a collisionally excited line of an ion of state X^{i+1} to a dielectronic recombination line from state X^i has a strong dependence on T_e (with $exp[-\Delta E/kT]$ being the energy difference between the two transition states above ground). Nussbaumer & Storey (1984) discuss this method in detail as applied to UV spectral lines, in addition to providing information on the relevant dielectronic recombination coefficients for various lines of C I, C II, C III, N I, N II, N III, N IV, O I, O II, O III, O IV, and O V. Some of the more commonly observable UV line ratios available for such purpose are (C III $\lambda 1908$)/(C II $\lambda 1335$), (C IV $\lambda 1549$)/(C III $\lambda 2297$ or $\lambda 977$), (N IV $\lambda 1486$)/(N III $\lambda 2064$ or $\lambda 991$), (N V $\lambda 1240$)/(N IV $\lambda 1719$), and (O IV $\lambda 1402$)/(O III $\lambda 835$). Unfortunately O I and O II do not have any significant dielectronic recombination lines in the UV to use with the UV O III] and [O II] lines. In addition, the UV dielectronic lines are usually weak in nebular spectra and their past use for T_e diagnostics (and abundances) have been limited to bright symbiotic stars (*cf.* Nussbaumer & Stencel 1987; Nussbaumer *et al.* 1988, and references therein).
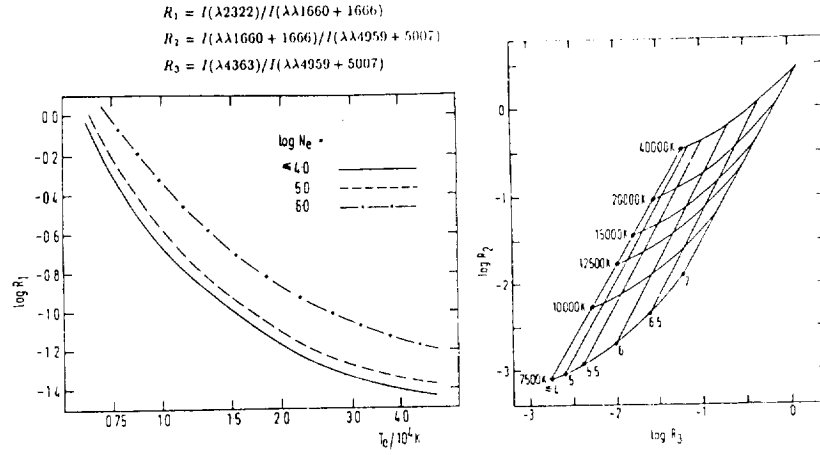
FIGURE 6. UV-intercombination/optical-forbidden line ratios of O III vs. T_e (*left*) and [O III] (auroral/nebular) (*right*) from Keenan & Aggarwal (1987).

4.3. Abundances

In addition to being probes of physical conditions in various ionization zones of astrophysical plasmas, UV emission lines provide fundamental data on abundances of the elements in the plasmas. Since abundances derived from emission lines is the topic of the review by M. Peimbert at this conference, I will limit my discussion to the impact that UV lines have in the field. Compared to ionic emission lines in optical spectra, the UV is unique in that it contains lines from abundant ions that have no optical counterparts: $C^{+,+2,+3}$, $N^{+2,+3,+4}$, $O^{+3,+4,+5}$, Ne^{+3}, $S^{+3,+4}$, $Mg^{+,+4}$, $Si^{+,+2,+3}$, $Al^{+,+2}$, and $Fe^{+3,+5}$. Included among these are the astrophysically important elements C, N, O, Mg, Si, and Fe for which determining abundances of is fundamental to understanding stellar nucleosynthesis processes and galactic chemical evolution. During the decade of the 1980's UV spectra of numerous emission-line objects were made with the IUE satellite which enabled the first comprehensive determination of abundances of C, N, Mg, and Si in a wide variety of objects ranging from comets to AGN (*cf.* the various reviews in Kondo 1987).

Traditionally two approaches have been applied to calculating abundances in nebular plasmas: (a) direct calculation of ionic abundance ratios from line strengths and applying empirical ionization corrections to get net elemental abundances, and (b) varying abundances (and other input parameters) in a photo-or shock-ionization model until a match to the observed spectrum is found. Aspects of the model approach is discussed in the review by G. Ferland at this conference, so I will limit my discussion to aspects of direct calculations of nebular abundances from UV emission lines. The vast majority of UV emission lines observed arise from collisional excitation or recombination (normal and dielectronic) for which their emissivities (eqns. 4 & 6) are functions of T_e, N_e, and ionic number density $N(X^i)$. The ratio of number densities of two ions follow from the ratio of two emission lines as:

$$\frac{N(X_k)}{N(X_l)} = \frac{I_{obs}(\lambda_k)}{I_{obs}(\lambda_l)} \frac{j(\lambda_l)}{j(\lambda_k)} = \frac{I_{obs}(\lambda_k)}{I_{obs}(\lambda_l)} \times f(\text{atomic data}, N_e^k, N_e^l, T_e^k, T_e^l), \qquad (8)$$

where the I_{obs}'s are the observed line intensities and the j's are the line emissivities. Note that on the right side of eqn. (8) "f" represents the functional dependence of the emissivities to atomic data (collision strengths, transition probabilities, wavelengths, and various constants) and the electron temperatures and densities *appropriate to the zones in a nebula where each of the two ions exist.*

It has been common practice to relate ionic abundances to hydrogen and calculate $N(X)/N(H^+)$ from UV-optical-IR line intensities relative to Hβ. For such purposes, Aller (1984) provided coefficients for deriving ionic abundances of 13 ions relative to H^+ that have prominent collisionally excited lines in the UV. His formulae are based on the assumption of an isothermal nebula of sufficiently low density where collisional deexcitation is negligible $(N_e < 10^4 cm^{-3})$ and are based on the compilation of atomic data by Mendoza (1983). They are applicable for most photoionized nebulae and emission-line galaxies of low to moderate density. However, care should be exercised in their use since newer atomic data are available for many of the ions and at high densities dielectronic recombination and radiative transfer problems for some of the UV resonance lines (*e.g.* C IV $\lambda1549$ and N V $\lambda1240$) become important.

Another procedure to perform calculations of ionic abundances, as well as T_e and N_e diagnostics from UV-optical-IR lines is to use a code that solves the statistical balance equation (eqn. 1) to get level populations and line emissivities for a specified (T_e, N_e), then use eqn. 8 with the observed line intensities to derive ionic abundance ratios. For most ions of astrophysical interest, a 5-level approximation is adequate and such a code has been developed and exported by De Robertis, Dufour, & Hunt (1987). During the past year, R. A. Shaw at ST ScI and the author have been upgrading this code with modern atomic data and including additional ions of particular importance in the UV (C II, C III, N III, O IV, and Si III). The code has been integrated into STSDAS/IRAF and is available with the current release of STSDAS (Shaw & Dufour 1993, 1994). While the original FIVEL code of De Robertis *et al.* was an interactive FORTRAN code, the new NEBULAR package has both interactive and automated options, where one can either input line ratios to derive T_e or N_e or ionic abundance ratios; or input a table of *observed* UV-optical line strengths and the program will perform reddening corrections using the Galactic extinction law of Seaton (1979), derive T_e and N_e from numerous ionic line ratios, construct a "diagnostic diagram" of $logN_e$ vs. $log T_e$, decide whether the data permits a 3-, 2-, or 1-zone (T_e, N_e) model (with the zones based on ionization potentials of various ions), then derive ionic abundances for most ions with UV or optical emission lines. Information about obtaining and using the program can be obtained via email to Dick Shaw at ST ScI (shaw@stsci.edu). We are continuously in the process of upgrading the program to include more ions as new atomic data becomes available, and plan in the future to add alternative reddening laws (*e.g.* LMC & SMC laws), include recombination lines of He I and He II, and improve the graphical and user-friendly aspects of the program.

While ionic abundance ratios are derivable directly from line intensity ratios, deriving total elemental abundance for some elements require corrections for ionic states without observable lines. Such corrections involve "empirical ICF's" (ionization correction factors) based on directly observed ionic ratios such as O^+/O^{+2} or ionization fractions computed by models. Optical spectra alone provide only a few ionic ratios for such purpose (*e.g.* O^+/O^{+2}, S^+/S^{+2}, Ar^{+2}/O^{+3}), while UV spectra provide a wealth of additional ionic ratios, particularly for high ionization objects. A good example is nitrogen, for which optical spectra contain only [N II] $\lambda\lambda6548,83$ - nominally indicative of only a small fraction of the total N abundance. By contrast, UV spectra contain prominent lines of N III], N IV], and N V which represent a large fraction of the existing states of N

in most nebular plasmas. Carbon is an even more extreme example, for which optical spectra provide only the C II λ4267 recombination line in any strength, while UV lines of C II], C III], and C IV exist which nominally represent a large fraction of the existing gaseous-phase carbon. In addition, C abundances derived from the (generally weak) C II λ4267 line for planetary nebulae have generally been much higher than from the UV lines (*cf.* Barker 1991 and references therein). An excellent discussion of the C abundance problem in PN has been presented by Rola & Stasińska (1994), who conclude that much of the discrepancy between the optical C II and UV C III] results is due to observational errors and selection effects with the weak optical C II line. Silicon is another element where deep UV spectra provide direct determination of the abundances of a majority of its existing ionic states and for which optical spectra have no significant lines.

4.4. *Extinction*

Corrections for interstellar extinction is a "necessary evil" in studies of UV spectra, particularly when comparisons have to be made to optical and infrared spectra. Fortunately the UV contains recombination lines of He I and He II which are relatively insensitive to T_e and N_e and facilitate both the determination of the magnitude and wavelength dependence of extinction for many types of objects. The stronger UV He I lines are of the triplet series, $2s^3S \rightarrow np^3P^\circ$, at 2663Å, 2696Å, 2733Å, 2763Å, 2829Å, 2945Å, and 3188Å, which can be compared to optical triplet and singlet lines such as those at 5876Å, 4471Å, 4026Å, 4921Å, and 6678Å. High excitation objects have strong UV lines of He II such as the Bα 1640Å line and Paschen series lines at 2253, 2306, 2511, 2733, and 3203 Å, which can be compared to He II Pα 4686Å and other optical He II lines. Seaton (1979) performed such a study of the heavily reddened planetary nebula NGC 7027 and developed an analytical "mean Galactic extinction curve" which has been widely used in nebular UV spectroscopy of Galactic objects. In addition to the recombination lines, collisionally excited metastable multiplet UV lines with optical counterparts can be used for extinction determinations (*e.g.* [O II], [O III], [Ne III], [Ar IV], and [Ne V]; Aller 1984), though the theoretical UV-optical line ratios are normally very sensitive to T_e.

Whenever practical, UV spectroscopy studies should evaluate both the magnitude and wavelength dependence of extinction from UV-optical emission-line comparisons. It is well established that the UV extinction along high-density lines of sight in the Galaxy (*e.g.* Mathis 1989), such as in the Orion Nebula, show significant deviations from the standard Galactic law of Seaton (1979) or Cardelli *et al.* (1989). In addition, the UV extinction in the LMC (Clayton & Martin 1985; Fitzpatrick 1985) and SMC (*e.g.* Nandy *et al.* 1982) shows variations, particularly in the relative weakness of the 2175Å bump and a steeper rise in the far UV for galaxies of lower metallicity than the Milky Way. Variations in extinction among Local Group spirals such as M31 and M33 has also been found (Hutchings *et al.* 1992) based on IUE spectroscopic studies.

5. Some recent UV emission-line studies with HST, HUT, & IUE

Since 1990 several UV spectroscopy studies of emission-line nebulae and galaxies have appeared in the literature based on observations with HST FOS & GHRS and the HUT spectrometer flown during the Astro-1 shuttle mission. In the remainder of this paper I will describe several of the excellent results obtained with these new-generation UV spectroscopy instruments.

5.1. *H* II *regions*

UV spectroscopy of Galactic and extragalactic H II regions provide the best means of determining the abundance of carbon in the ISM of galaxies via the C III] λ1909 and C II] λ2325 emission lines. The IUE has been used extensively for such studies (*cf.* Dufour 1987), with recent analyses of CNO abundances in the Orion Nebula (Walter, Dufour, & Hester 1992) and the Lagoon Nebula (Peimbert, Torres-Peimbert, & Dufour 1993) reported. In addition, Rubin, Dufour, & Walter (1993) reported the first analysis of Si-C abundances in an H II region (Orion) using high dispersion IUE observations. These and previous studies indicate that C/O is approximately solar in M42 and M8, but that temperature fluctuations in an H II region need to be evaluated carefully for accurate determination of C abundances from the UV lines. In addition, Rubin *et al.* 1993 found the gaseous-phase Si (from the UV Si III] lines) abundance to be significantly depleted (Si/H ∼ 1/8 solar) in Orion. Studies of extragalactic H II regions with IUE generally indicated that C/O decreases with O/H in the ISM of metal-poor systems, but that C/N∼constant (Dufour 1988).

Observations of the UV emission-line spectra of H II regions with the IUE are limited in S/N and resolution due to the limited dynamic range of its vidicon detectors and spectral impurity by the extended objects filling the large aperture. Observations of several extragalactic H II regions with the HST FOS have been recently conducted during Cycles 2 & 3 with excellent results. A comparison of HST FOS and IUE low dispersion UV spectra of SBS 0335-052 and 30 Doradus in the LMC has been presented by Dufour *et al.* (1993), which illustrate vividly how the higher dynamic range and better resolution of FOS permits ten-fold improvements in S/N of various weak emission lines compared to what is possible with IUE. Poster papers of FOS spectra of the Orion Nebula (Rubin *et al.* 1994) and the Lagoon Nebula (Cox 1994) are presented at this conference. In addition, a poster comparing HST GHRS spectra of the C II] λλ2325 multiplet in Orion with IUE high dispersion data is presented by Walter *et al.* (1994).

An illustration of the excellent S/N and resolution afforded by HST FOS UV spectra of H II regions, Figure 7 presents spectra of the Orion Nebula and SMC N88A (an H II region in the Small Magellanic Cloud) over the 1150–3200Å wavelength range. The two spectra illustrate the various emission lines which can be seen in a moderate excitation metal-rich and dusty Galactic H II region (Orion) compared to an high excitation metal-poor extragalactic H II region (N88A). Despite the spectra being rebinned for display and smoothed by a 3-point gaussian, the high resolution of the "low dispersion" FOS spectra is evident, with the multiplets of O III] λλ1663, Si III] λλ1888, and C II] λλ2325 being partially or cleanly resolved. This higher resolution available on FOS spectra of H II regions is very important for detection and measurement of emission lines above the usually strong UV continuum in H II regions (due to scattering by dust or inclusion of hot stars in the aperture). Another significant advantage of FOS spectra is that longer wavelength optical-nearIR spectra can be obtained with the same aperture as the UV spectra, thus enabling accurate comparisons of spectral lines over a broad wavelength range. One of the historical problems with IUE spectra of extended sources has been the "tie-in" between UV spectral measurements with optical spectra due to the usually different aperture sizes and orientations used. This problem is most evident in carbon abundances derived (from C III] λλ1909) for the most metal-poor galaxy known, IZw18 (Dufour, Garnett, & Shields 1988; Dufour & Hester 1990), where imagery data is necessary to accurately tie-in the IUE UV and optical line measurements.

The impact that the high quality UV spectra of H II regions now possible with HST FOS will have on the problem of CNO (and Si) abundances and chemical evolution is
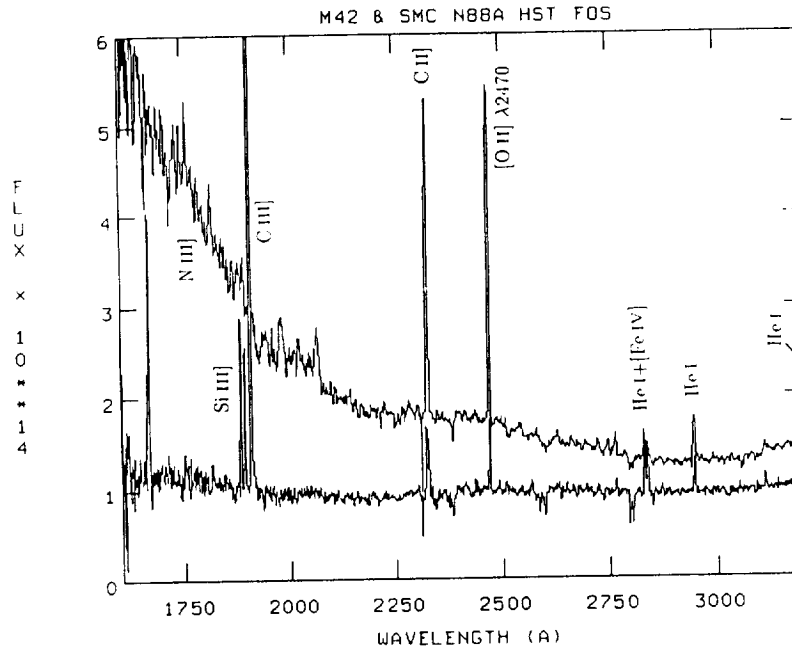
FIGURE 7. HST FOS spectra of two H II regions in the 1600-3300Å region (gratings G190H & G270H): M42 (Orion Nebula, *top*) and SMC N88A (a compact high excitation H II region in the Small Magellanic Cloud, *bottom*).

evident from the study of C/O abundance variations in seven extragalactic H II regions by Garnett *et al.* (1994). HST FOS spectra were obtained with the G190H grating, which enabled measurement of both the C III] 1909Å and O III] 1663Å lines and direct determination of the C^{+2}/O^{+2} in a manner that is insensitive to T_e, N_e, and extinction corrections. Their results for C/O and C/N, the latter based on optical measurements of [N II] 6583Å and nebular model ICF's, are shown in Figure 8. They found that C/O increases with O/H, consistent with a power law having an index of 0.43 ± 0.09 over the range of $-4.7 \leq \log(O/H) \leq -3.6$. In addition, unlike previous studies, they found that C/N increases with O/H in irregular galaxies, but is lower for solar neighborhood stars and H II regions. This suggests that the most metal-poor galaxies support the idea that their ISM enrichment is only from massive stars, while that of more metal-rich systems, like the Galaxy, have higher C/O due to a delayed enrichment from intermediate mass stars. They interpret the C/N results as indicating that the bulk of the nitrogen production is decoupled from the synthesis of carbon in the Galaxy. The Garnett *et al.* spectra also provide more accurate determination of Si/C and Si/O in metal-poor H II regions than previously possible (from the cleanly resolved Si III] and C III] lines, and detection of O III] in the UV), and the preliminary analysis (Dufour *et al.* 1994) suggest that the gaseous-phase Si/O ratio in the H II regions is generally lower than solar by a factor of $\sim$2-3.

FIGURE 8. The variation of C/O (*left*) and C/N (*right*) for extragalactic H II regions, based on HST FOS observations by Garnett *et al.* (1994).

5.2. Planetary Nebulae

During it history, the IUE satellite has made extensive observations of the UV spectra of planetary nebulae (PNe), with ~2800 spectra currently existing in the archives. Since numerous Galactic PNe are bright and have relatively low extinction, the IUE has enjoyed excellent success in obtaining PN spectra (as well as of their central stars) at both low and high dispersion. UV emission-line spectra of PNe span a large range in their ionization characteristics, as is evident from the *IUE Spectral Atlas of Planetary Nebulae, Central Stars, and Related Objects* by Feibelman *et al.* (1988). A review of their UV spectral characteristics and early scientific results of IUE studies of PNe has been given by Köppen & Aller (1987). UV spectroscopy of PNe and of their central stars permit: (a) additional T_e and N_e diagnostics to be made from UV-line multiplets, particularly for the high ionization inner zones of the shells; (b) improved abundance determinations of certain elements, most importantly of C, N, Si, and Mg which have few or no optical lines; (c) evaluation of dielectronic recombination effects for lines of C III, C IV, N IV], N V, O III], O IV], etc.; (d) evaluate internal extinction and optical depth effects in resonance lines; (e) permit determination of effective temperatures and mass-loss rates for their central stars; and (f) provide additional constraints on physical parameters necessary for realistic theoretical models of PNe to be developed.

The most extensive study of PNe abundances from modern UV-optical spectra is by Perinotto (1991). He compiled data on 209 Galactic PNe and studied correlations between He, C, N, O, and Ne, and compared the results to the expectations of modern stellar evolution and nucleosynthesis theory for intermediate-mass stars. Perinotto concluded that the enrichment of N in type I PNe (He- & N-rich PNe arising from the more massive progenitors) is due mostly to the ON cycle, while that for type II–III PNe is due to the CN cycle.

The IUE has also had success in studying the spectra of extragalactic PNe, particularly in the Magellanic Clouds (*cf.* the review by Dufour 1990 and spectra of 5 SMC and 6 LMC PNe in the Feibelman *et al.* 1988 atlas), where it is possible to assess the effects of C-N enrichment in PN from low metallicity progenitors. Many PN in the Clouds were found to have significant enrichments of C and N compared to that in H II regions (Aller *et al.* 1987), suggesting that the shell compositions reflect the products of the third

dredge-up phase of intermediate-mass star AGB evolution, where primary carbon from the core is ejected into the RG envelope prior to PN formation. If so, then PNe from intermediate-mass stars could be an important factor in C and N-enrichment during the early chemical evolution of galaxies.

To date (mid-1994), little has appeared in the refereed literature regarding HST and HUT observations the UV spectra of PNe. The first reported FOS study was by Dopita *et al.* (1994) of the low-excitation planetary nebula SMP 85 in the LMC; which they found to be a dense, young, carbon-rich object—being only about 500–1000 years in time since ionization began. It is likely that the future will see HST FOS, and possibly GHRS, observation of the UV spectra of more PNe, most likely faint and small extragalactic objects, Galactic Halo PNe, and possibly a few Galactic PNe of special scientific interest. The only PNe the author knows of observations were made by HUT was NGC 1535, for which spectra were obtained on and off the central star (Bowers *et al.* 1994). The spectrum of the central star is interesting in that the UV O VI 1035Å, N V 1240Å, and O V 1375Å lines all showed strong P-Cygni line profiles indicating their origin in the immediate vicinity of the star (all were weak or absent in the spectrum off the star).

5.3. *Supernova remnants*

The UV spectra of supernova remnants (SNRs) are rich in emission lines due to the high temperatures and ionization levels associated with the shocked gas. Studies of the many UV emission-line diagnostics nominally present provide important measurements of the shock and post-shock conditions in the gas. SNRs have been extensively observed with IUE, with the Cygnus Loop and Crab Nebula being the favorite Galactic SNRs (due to low extinction and large angular size), followed by SNRs in the LMC (*cf.* the review by Blair & Panagia 1987). In particular, the Cygnus Loop has been the target of extensive studies by the IUE (spectra of several positions) coupled with multi-wavelength spectral and imagery data and spatial model analyses (*e.g.* Raymond *et al.* 1988; Hester, Raymond, & Blair 1994) to assess in detail the complex nature of the shocked ISM structures visible. The Far-UV (FUV) region also contains several high-excitation UV lines important for SNR shock diagnostics; among the most important is O VI at 1032+38Å, for which Raymond *et al.* (1983) noted is the dominant line energy loss mechanism in the post-shock flow. FUV spectrophotometric observations of the Cygnus Loop have been made with the VOYAGER 1 & 2 spacecraft (Shemansky, Sandel, & Broadfoot 1979; Vancura *et al.* 1993), with the second study detecting C III 977Å, O VI 1035Å, and Lyα 1215Å.

SNRs were high-priority targets for HUT during the Astro-1 mission and observations for three have been reported in the literature: the Cygnus Loop (Blair *et al.* 1991; Long *et al.* 1992), the Crab Nebula (Blair *et al.* 1992), and N49 in the LMC (Vancura *et al.* 1992b). The spectra obtained for two filaments in the Cygnus Loop are shown in Figure 9 (kindly provided to the author by W. P. Blair). Comparison of the two spectra is very interesting in that the radiative filament shows emission lines from several ionic states of C, N, and O; while the spectrum of the nonradiative filament is dominated by O VI λλ1032+1038, which is partially resolved, as well as other high ionization species due to the higher shock velocity and relative greater incompleteness compared to the radiative filament. Blair *et al.* (1991) modeled the radiative shock spectrum and concluded that it is dominated by a fast $v \sim 165$ km s^{-1} incomplete shock, but slower shocks may contribute to the observed spectrum. The nonradiative filament spectrum was discussed and modeled by Long *et al.* (1992), who concluded that much of the FUV-UV spectrum is consistent with a shock of velocity 175–185 km s^{-1} propagating into a low density
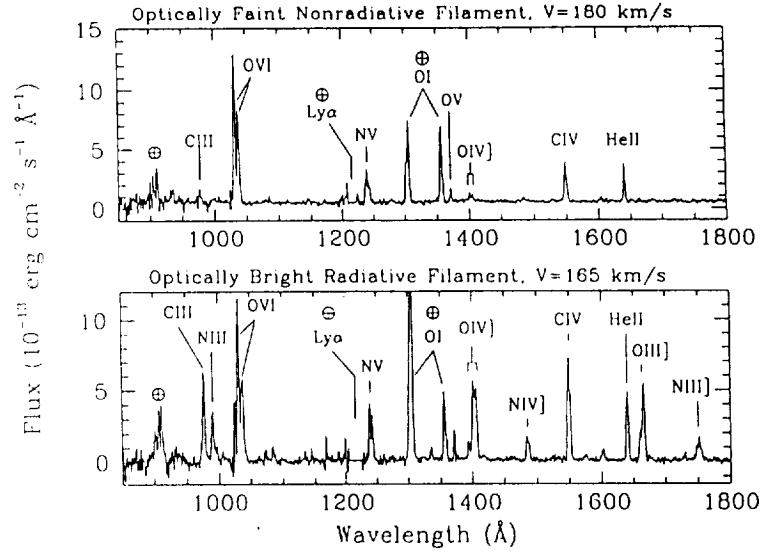
FIGURE 9. HUT FUV-UV spectra of two filaments in the Cygnus Loop SNR. The top spectrum (Blair *et al.* 1991) is of a high velocity nonradiative filament with a very incomplete recombination zone, while the bottom spectrum (Long *et al.* 1992) is of a slower radiative filament which is more complete.

medium, but that lower shock velocities indicated by optical Hα profiles suggest that the shock is rapidly decelerating as it encounters denser material.

The HUT spectrum of the LMC SNR N49 (Vancura *et al.* 1992b) showed emission lines of O VI λλ1035, O IV] λλ1402, C IV λλ1549, and He II λ1640 from the remnant. They interpreted the HUT spectral results based on a model for N49 previously developed from a multiwavelength (IUE UV spectra, ground-based imagery and spectroscopy, and Einstein X-ray imagery) study (Vancura *et al.* 1992a). The most useful diagnostic from the HUT spectrum was O VI λλ1035Å, which they note as originating in faint low density shocks with $v \sim 190$–270 km s^{-1} tranversing clouds with $n \sim 20$–40 km s^{-1}, rather than in the main $v \sim 730$ km s^{-1} blast wave of the remnant. They presented a shock model with a distribution of shock velocities to match well the entire FUV-UV-optical spectral line strengths observed. By contrast, the Crab Nebula spectrum showed few FUV emission lines, but showed a heavily reddened synchrotron continuum down to $\lambda \sim 1000$Å with only two emission lines, C IV λλ1549 and He II λ1640, detected. The C IV line showed a double-peaked profile, representative of the two sides of an expanding shell of velocity $v_{exp} \sim \pm 1100$ km s^{-1}; while the He II line showed only one blueshifted component representative of the near side of the shell.

5.4. Emission-line galaxies

During its 15+ years of operation, the IUE has obtained over 5000 UV spectra of AGN and starburst galaxies. A summary of most of the principal studies during the first half of this period can be found in the reviews of "Starburst Galaxies," "Active Galactic Nuclei," "Blazars," and "Quasars" in *Exploring the Universe with the IUE Satellite* (Kondo 1987). In recent years much attention has been given to using the large IUE UV spectra database for the construction of atlases of the various types (*cf.* Table 2),
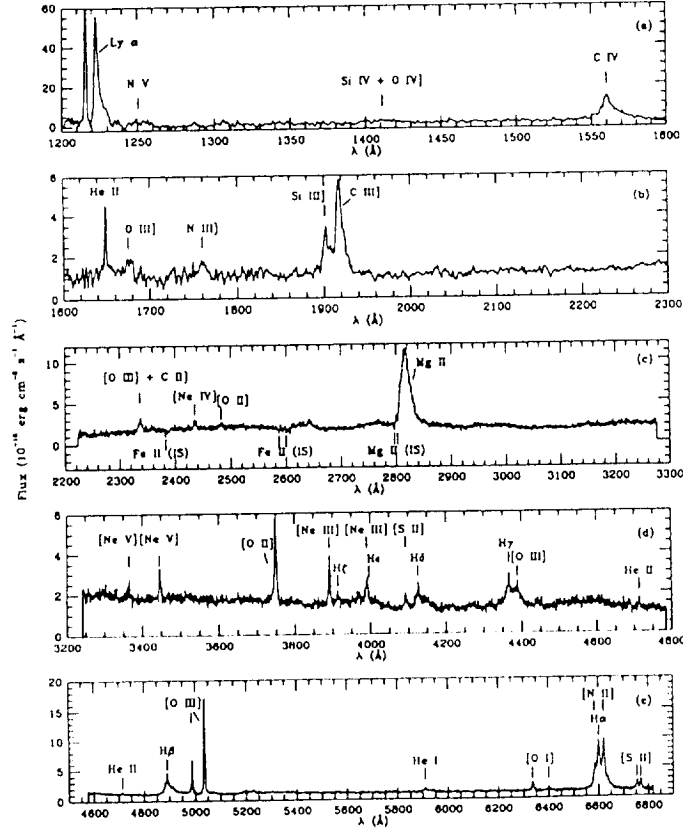
FIGURE 10. HST FOS spectra of the weak Seyfert 1 nucleus of NGC 1566 from Kriss *et al.* (1991) illustrating complete UV-optical spectral coverage capabilities of FOS over 1150–6800Å.

UV broad-line region variability studies (*e.g.* Clavel *et al.* 1991; Koratkar & Gaskell 1991 for NGC 5548; Zheng, Fang, & Binette 1992 for Fairall 9; Reichert *et al.* 1994 for NGC 3783), studies of the Baldwin Effect in Quasars (Kinney, Rivolo, & Koratkar 1990), and development of a new classification scheme for QSO's based on combined UV-optical spectral characteristics (Francis *et al.* 1992). In addition, numerous UV spectral studies of individual objects made with the IUE continue to appear in the literature. Among the more innovative use of IUE large aperture spectra has been to utilize the fact that the 10″ × 20″ large aperture *images* extended objects in UV emission lines and the 2D line features in low dispersion spectra can be deconvolved to spatially map the emission structure. This technique has been applied to resolve emission knots in the Seyfert galaxy NGC 1068 (Bruhweiler & Altner 1988) and study the spatial distribution of emission in the core of the LINER galaxy NGC 3998 (*e.g.* Reichert *et al.* 1992). It is expected that the NEWSIPS-processed low dispersion IUE archive with its improved geometric processing will enable improved UV emission-line maps of extended objects to be made in the future.

Even with the aberration problem, HST FOS and GHRS UV spectra of the central regions of various emission-line galaxies have been successful. Among the first objects to be studied by FOS included the Quasar UM 675 (Beaver *et al.* 1991), 3C 273 (Bahcall *et al.* 1991), the nucleus of NGC 1068 (Caganoff *et al.* 1991), and the weak Seyfert galaxy NGC 1566 (Kriss *et al.* 1991). More recently, as HST comes into more "routine" operation, multi-object UV spectroscopy studies of AGN have appeared in the literature (*e.g.* Laor *et al.* 1994). In addition to having high sensitivity and large dynamic range, FOS has the capability of taking spectra of sub-arcsecond regions in and near AGN covering a wide UV-optical wavelength range. An example of such high quality spectra for NGC 1566 from Kriss *et al.* is shown in Figure 10. Such spectra enable UV-optical emission-line diagnostics, including velocity profiles, to be made of the stellar cores of AGN without significant contamination by emission from adjacent sources. An even more difficult problem (due to the relatively much more luminous nuclear region) is to study the spectra of regions near the central source in AGN, one of the first results from GHRS was obtaining a high resolution UV spectrum, covering the 1150–1450Å & 1490–1750Å wavelength range, of a starburst knot near the nucleus of NGC 1068 (Hutchings *et al.* 1991). The spectrum indicated that the knot consisted of thousands of OB stars which were formed only $\sim$ 3 million years ago. Now with the correction afforded to FOS and GHRS by COSTAR, such studies are now even more practical for AGN and other types of emission-line nuclei of galaxies.

Among the most successful of the HUT observations during the Astro-1 mission were FUV-UV spectra of the Seyfert galaxies NGC 4151 (Kriss *et al.* 1992a) and NGC 1068 (Kriss *et al.* 1992b). The NGC 1068 FUV-UV spectrum is reproduced in Figure 11. Kriss *et al.* noted that the FUV lines of C III 977Å, N III 991Å, and O VI 1035Å were found to be stronger than expected. T_e's derived from the ratios of the FUV lines of C III and N III to the UV intercombination lines of C III] 1909Å and N III] 1750Å, were 26,700 K and 24,000 K, respectively. These high values and the very strong O VI line led them to conclude that shock heating is an important mechanism in the nucleus of NGC 1068. By contrast, the FUV lines of C III and N III appear in *absorption* (blueshifted by about 200–1330 km s^{-1}) in the nucleus of NGC 4151 and the O VI lines have both emission and blueshifted absorption components. Other emission lines, such as C IV 1549Å, had narrow emission, blueshifted narrow absorption, and broad emission wings. They concluded that the spectral features were consistent with high density ($n \sim 10^{9.5}$ cm^{-3}) outflowing material from the broad-line region.

6. CONCLUDING REMARKS

The author wishes to express his gratitude in being invited to present a review paper on "UV Spectroscopy" a conference honoring two pioneers in the field of emission-lines of astrophysical plasmas—Don Osterbrock and Mike Seaton. To Don I owe the gratitude of a son, since he fathered me into the field of nebular spectroscopy as his 13th (lucky!) Ph.D. student at Wisconsin and for continual motivation to continue my studies in the two decades since. To Mike I owe almost an equivalent gratitude for fathering many of the "young turks" of modern atomic physics who are now providing me and other spectroscopists modern atomic data for use in our analyses.

The present and the future is bright for us in the field of UV spectroscopy. The IUE continues to acquire *scientifically important* UV spectra of all kinds of astronomical objects and the astronomical community needs to keep the pressure on NASA to continue support of its operation. HST is "fixed" and continues the promise of acquiring UV spectra of exceptional quality of many faint objects not previously reachable with IUE in
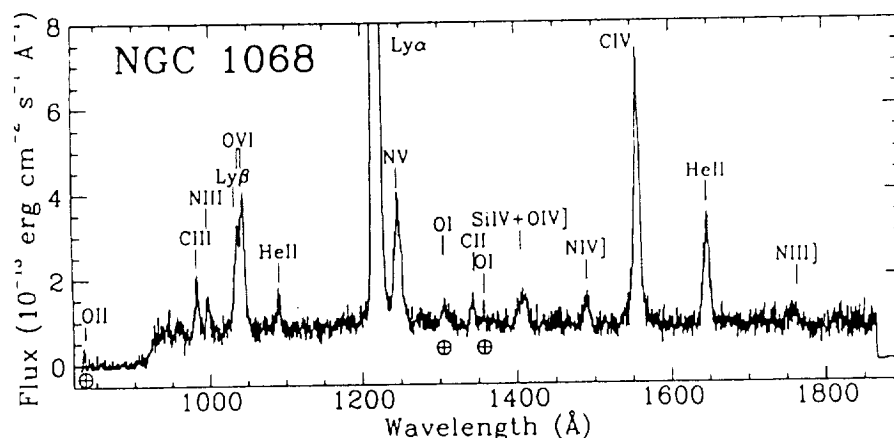
FIGURE 11. HUT FUV-UV spectrum of the nucleus of the Seyfert 1 galaxy NGC 1068 from Kriss *et al.* (1992b). Note the strong O VI 1035Å line, which Kriss *et al.* argues as being indicative of shock ionization in the nucleus.

the coming decade (as well as offering the promise of being able to obtain 2D spectra later in the decade). HUT has obtained high quality spectra in the FUV during the Astro-1 mission and we hope for even more success for it during the 1995 Astro-2 mission. EUVE is now in the middle of its lifespan with exciting results for the EUV region only now coming out in press. The promise of Lyman for enabling us to have an extended future of being able to do EUV-FUV spectroscopy by an orbiting spacecraft, potentially as versatile as IUE, is important to all of us and we should continue to urge its strong support by NASA.

REFERENCES

ALLER, L. H. 1984 *Physics of Thermal Gaseous Nebulae*, Dordrecht: Reidel

ALLER, L. H. *et al.* 1987 *ApJ* **320**, 159

AUFDENBERG, J. P. 1993 *ApJS* **87**, 337

BAHCALL, J. N. *et al.* 1991 *ApJL* **377**, L5

BARKER, T. 1991 *ApJ* **371**, 217

BEAVER, E. A. *et al.* 1991 *ApJL* **377**, L1

BENVENUTI, P. *et al.* 1982 NASA SP-1046

BLAIR, W. P. & PANAGIA, N. 1987 in *Exploring the Universe with the IUE Satellite* (ed. Y. Kondo) Dordrecht: Reidel, p. 549

BLAIR, W. P. *et al.* 1991 *ApJL* **379**, L33

BLAIR, W. P. *et al.* 1992 *ApJ* **399**, 611

BLUM, R. D. & PRADHAN, A. K. 1992 *ApJS* **80**, 425

BOGGESS, A. et al. 1978 *Nature* **275**, 372

BOWYER, S. 1994 *Science* **263**, 55

BOWERS, C. W. et al. 1994 in preparation.

BRANDT, J. C. et al. 1994 *PASP* **106**, 890

BRUHWEILER, F. C. & ALTNER, B. 1988 in *A Decade of UV Astronomy with the IUE Satellite*, Vol. 2, (ed. E. J. Rolfe) Noordwijk: ESTC, 319

CAGANOFF, S. et al. 1991 *ApJL* **377**, L9

CARDELLI, J. A., CLAYTON, G. C. & MATHIS, J. S. 1989 *ApJ* **345**, 245

CLAVEL, J. et al. 1991 *ApJ* **366**, 64

CLAYTON, G. & MARTIN, P. 1985 *ApJ* **288**, 558

CODE, A. D. (ed.) 1972 *The Scientific Results from the Orbiting Astronomical Observatory (OAO-2)*, NASA SP-310

COX, N. 1994 poster paper, this conference

CZYZAK, S. J., KEYES, C. D. & ALLER, L. H. 1986 *ApJS* **61**, 159

DAVIDSEN, A. F. et al. 1992 *ApJ* **392**, 264

DeROBERTIS, M. M., DUFOUR, R. J. & HUNT, R. W. 1987 *JRASC* **81**, 195

DOPITA, M. A. et al. 1994 *ApJ* **426**, 150

DOSCHEK, G. A. & FEIBELMAN, W. A. 1993 *ApJS* **87**, 331

DOYLE, J. G. & KEENAN, F. P. 1992 *AAp* **264**, 173

DUFOUR, R. J. 1986 *PASP* **98**, 1025

DUFOUR, R. J. 1990 in *Evolution in Astrophysics*, (ed. E. J. Rolfe), ESA SP-310, p. 117

DUFOUR, R. J. 1991 *PASP* **103**, 857

DUFOUR, R. J., GARNETT, D. R. & SHIELDS, G. A. 1988 *ApJ* **332**, 752

DUFOUR, R. J. & HESTER, J. J. 1990 *ApJ* **350**, 149

DUFOUR, R. J. et al. 1993 *RMAA* **27**, 115

DUFOUR, R. J. et al. 1994 in preparation

EDELSON, R. et al. 1992 *ApJS* **83**, 1

FEIBLEMAN, W. A. 1994 *PASP* **106**, 756

FERLAND, G. J. & OSTERBROCK, D. E. 1986 *ApJ* **300**, 658

FITZPATRICK, E. L. 1985 *ApJ* **299**, 219

FRANCIS, P. J. et al. 1992 *ApJ* **398**, 476

GARNETT, D. R. et al. 1994 *ApJ* in press

HARRINGTON, J. P., SEATON, M. J., ADAMS, S. & LUTZ, J. H. 1982 *MNRAS* **199**, 517

HARRIS, A. W. & SONNEBORN, G. 1987 in *Exploring the Universe with the IUE Satellite* (ed. Y. Kondo) Dordrecht: Reidel, p. 729

HAYES, M. A. & NUSSBAUMER, H. 1986 *A&Ap* **161**, 287

HESTER, J. J., RAYMOND, J. C. & BLAIR, W. P. 1994 *ApJ* **420**, 721

HECK, A., EGRET, D., JASCHEK, M. & JASCHEK, C. 1984 IUE Low-Resolution Spectra Atlas: Part 1. Normal Stars, ESA SP-1052.

HUTCHINGS, J. B. et al. 1991 *ApJL* **377**, L25

HUTCHINGS, J. B. et al. 1992 *ApJL* **400**, L35

KEENAN, F. P. & AGGARWAL, K. M. 1987 *ApJ* **319**, 403

KEENAN, F. P., FEIBELMAN, W. A. & BERRINGTON, K. A. 1992 *ApJ* **389**, 443

KEENAN, F. P. et al. 1994 *ApJ* **423**, 882

KINNEY, A. L., BOHLIN, R. C., BLADES, J. C. & YORK, D. G. 1991 *ApJS* **75**, 645

KINNEY, A. L. et al. 1993 *ApJS* **86**, 5

KINNEY, A. L., RIVOLO, A. R. & KORATKAR, A. P. 1990 *ApJ* **357**, 338

KONDO, Y. (ed.) 1989 *Exploring the Universe with the IUE Satellite*, Dordrecht: Reidel

KÖPPEN, J. & ALLER, L. H. 1987 in *Exploring the Universe with the IUE Satellite* (ed. Y. Kondo) Dordrecht: Reidel, p. 589

KORATKAR, A. P. & GASKELL C. M. 1991 *ApJ* **375**, 85

KRÄMER, G. *et al.* 1990 in *Observatories in Earth Orbit and Beyond* (ed. Y. Kondo) Dordrecht: Kluwer, p. 177.

KRISS, G. A. *et al.* 1991 *ApJL* **377**, L13

KRISS, G. A. *et al.* 1992a *ApJ* **392**, 485

KRISS, G. A., DAVIDSEN, A. F., BLAIR, W. P., FERGUSON, H. C. & LONG, K. S. 1992b *ApJL* **394**, L37

LANZETTA, K. M., TURNSHEK, D. A. & SANDOVAL, J. 1993 *ApJS* **84**, 109

LAOR, A. *et al.* 1994 *ApJ* **420**, 110

LONG, K. S. *et al.* 1992 *ApJ* **400**, 214

MATHIS, J. S. 1989 *AnRevAAp* **28**, 37

MENDOZA, C. 1983 in *IAU Symp. No. 103: Planetary Nebulae* (ed. D. R. Flower) Dordrecht: Reidel, p. 143

MOOS, W. 1990 in *Observatories in Earth Orbit and Beyond* (ed. Y. Kondo) Dordrecht: Kluwer, p. 171

MORTON, D. C. & SPITZER, L. 1966 *ApJ* **144**, 1

NANDY, K. *et al.* 1982 *MNRAS* **201**, 1P

NICHOLS, J. S., GARHART, M. P., DE LA PEÑA, M. D. & LEVAY K. L. 1994 IUE Newsletter No. 53, 1

NUSSBAUMER, H. 1986 *AAp* **155**, 205

NUSSBAUMER, H., SCHILD, H., SCHMID, H. M. & VOGEL, M. 1988 *AAp* **198**, 179

NUSSBAUMER, H. & STENCEL, R. E. 1987 in Exploring the Universe with the IUE Satellite (ed. Y. Kondo) Dordrecht: Reidel, p. 203

NUSSBAUMER, H. & STOREY, P. J. 1984 *AApSup* **56**, 293

OSTERBROCK, D. E. 1989 *Astrophysics of Gaseous Nebulae and AGN*, Mill Valley: University Science Books

PEIMBERT, M., TORRES-PEIMBERT, S. & DUFOUR, R. J. 1993 *ApJ* **418**, 760

PENSTON, M. V. *et al.* 1983 *MNRAS* **202**, 833

PERINOTTO, M. 1991 *ApJS* **76**, 687

PITTS, P. S. 1993 IUE Newsletter No. 50, p. 21

RAYMOND, J. C., BLAIR, W. P., FESEN, R. A. & GULL, T. R. 1983 *ApJ* **275**, 636

RAYMOND, J. C. *et al.* 1988 *ApJ* **324**, 869

REICHERT, G. A. *et al.* 1992 *ApJ* **387**, 536

REICHERT, G. A. *et al.* 1994 *ApJ* **425**, 582

ROGERSON, J. B. *et al.* 1973 *ApJL* **181**, L97

ROLA, C. & STASIŃSKA, G. 1994 *AAp* **282**, 199

ROSA, M., JOUBERT, M. & BENVENUTI, P. 1984 *AApS* **57**, 351

RUBIN, R. H., DUFOUR, R. J. & WALTER, D. K. 1993 *ApJ* **413**, 242

RUBIN, R. H. *et al.* 1994 poster paper, this conference

SEATON, M. J. 1979 *MNRAS* **187**, 73P

SHAW, R. A. & DUFOUR, R. J. 1993 *ASP Conf. Ser.* Vol. 61, p. 327

SHAW, R. A. & DUFOUR, R. J. 1994 in preparation (to be submitted for publication in *PASP*)

SHEMANSKY, D. E., SANDEL, B. R. & BROADFOOT, A. L. 1979 *ApJ* **231**, 35

STAFFORD, R. P., BELL, K. L. & HIBBERT, A. 1994 *MNRAS* **266**, 715

STECHER, T. P. & MILLIGAN, J. E. 1962 *ApJ* **136**, 1

VANCURA, O., BLAIR, W. P., LONG, K. S. & RAYMOND, J. C. 1992a *ApJ* **394**, 158

VANCURA, O. *et al.* 1992b *ApJ* **401**, 220

VANCURA, O., BLAIR, W. P., LONG, K. S., RAYMOND, J. C. & HOLBERG, J. B. 1993 *ApJ* **417**, 663

WALTER, D. K. *et al.* 1994 poster paper, this conference

WALTER, D. K., DUFOUR, R. J. & HESTER, J. J. 1992 *ApJ* **397**, 196

WAMSTEKER, W. *et al.* 1989 *AApS* **79**, 1

WILLIAMS, R. E. 1994 poster paper, this conference.

WU, C.-C. *et al.* 1983 IUE Newsletter No. 22

WU, C.-C. *et al.* 1992 IUE Ultraviolet Spectral Atlas of Selected Astronomical Objects, NASA RP-1285

ZHENG, W., FANG, L.-Z. & BINETTE, L. 1992 *ApJ* **392**, 74